Materials Research Express

PAPER

RECEIVED
23 March 2017

REVISED
22 May 2017

ACCEPTED FOR PUBLICATION
31 May 2017

PUBLISHED
18 July 2017

Robust *p*-type doping of copper oxide using nitrogen implantation

Marina Jorge[1], Stanislav M Polyakov[1], Simon Cooil[1], Alex K Schenk[1], Mark Edmonds[2], Lars Thomsen[3], Federico Mazzola[1,4] and Justin W Wells[1,5]

[1] Department of Physics, Norwegian University of Science and Technology (NTNU), N-7491 Trondheim, Norway
[2] School of Physics and Astronomy and Monash Centre for Atomically Thin Materials, Clayton Victoria 3800, Australia
[3] The Australian Synchrotron, 800 Blackburn Road, Clayton, Victoria 3168, Australia
[4] Present address: School of Physics and Astronomy, University of St Andrews, St Andrews, Fife KY16 9SS, United Kingdom
[5] Present address: Department of Chemistry and Physics, La Trobe University, Melbourne, Australia

E-mail: quantum.wells@gmail.com

Keywords: Cu_2O, photovoltaics, N^+ implantation, photoemission

Abstract

We demonstrate robust *p*-type doping of Cu_2O using low/medium energy ion implantation. Samples are made by controlled oxidation of annealed Cu metal foils, which results in Cu_2O with levels of doping close to intrinsic. Samples are then implanted with nitrogen ions using a kinetic energy in the few keV range. Using this method, we are able to produce very high levels of doping, as evidenced by a 350 meV shift in the Fermi level towards the VB maximum.

The robustness of the nitrogen implanted samples are tested by exposing them to atmospheric contaminants, and elevated temperatures. The samples are found to survive an increase in temperature of many hundreds of degrees. The robustness of the samples, combined with the fact that the materials used are safe, abundant and non-toxic and that the methods used for the growth of Cu_2O and N^+ implantation are simple and cheap to implement industrially, underlines the potential of Cu_2O:N for affordable intermediate band photovoltaics.

1. Introduction

Copper oxide (Cu_2O) is an abundant non-toxic intrinsic *p*-type semiconductor [1], with a long exciton lifetime [2], low-cost producibility, and a direct band gap of 2.1 eV. It has therefore attracted much attention in the photovoltaic solar cell community [1]. However, the discrepancy between the theoretical efficiency (approaching 12% [3]) and the efficiency actually achieved with technologies available (<2% [4, 5]) resulted in a lack of further interest in Cu_2O as a possible photovoltaic material. Besides the low efficiency obtained, another major drawback of Cu_2O was the difficulty in controlling the electrical properties due to its intrinsic p-type conductivity as a result of copper vacancies [6]. More recently, there has been a resurgence of interest in Cu_2O as a photovoltaic. In 2016, the highest Cu_2O solar cell efficiency achieved had increased (to 8.1% [7]), but is still poor compared to competing materials.

Luque *et al* proposed a concept of intermediate band solar cells (IBSCs) which can solve the problem of low efficiency: with the creation of a partially filled band within the band gap, the electrons not only jump from the valence band (VB) into the conduction band (CB) by absorption of at least the energy of the band gap (E_g) as in single gap solar cells, but also lower photon energies are absorbed, allowing the transition of carriers from the VB into the CB by using the IB as a 'stepping stone'. Therefore, the Shockley–Queisser limit [8] is overcome, making theoretical conversion efficiencies of such solar cells up to 20% higher than single gap solar cells [9]. Several major strategies exist for creating IBSCs: including multiple quantum dots layers [10], doping with highly mismatched elements [11] or doping with a suitable element which forms delocalized energy levels in the band gap [12, 13] are all suggested as viable methods.

The need to control the electrical properties of Cu_2O translates into the need to select suitable elements with which dope the host material. Due to concerns of damaging or distressing the bulk host, and because it is not a standard industry method, ion implantation of high dopant densities is one of the least investigated methods of creating an IBSC [14]. Nevertheless, attempts to implant Cd, In and Cl in Cu_2O have been made, and have shown promise [15–17]. Nitrogen also appeared as a promising dopant option, not only for being nontoxic, low-cost and easily accessible, but also because it has a similar atomic radius to oxygen, and hence may be possible to substitute,

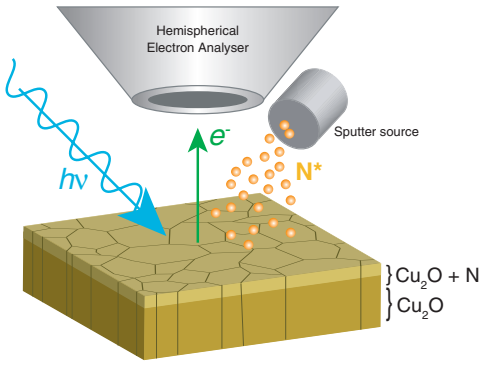

Figure 1. Schematic representation of a Cu_2O sample undergoing nitrogen implantation and XPS/UPS measurement.

whereupon is will act as an acceptor in Cu_2O. Studies focusing on doped Cu_2O:N, highlighted that it decreased the Cu_2O resistivity and created an acceptor level at 0.14 eV above the VB maximum [18]. Later, a concentration of 3% N was found to be concomitant with a widening of the band gap [19], to a value of 2.52 ± 0.03 eV [20]. A nitrogen doping density of 2.5% has also been reported, once again confirming the reduction of the resistivity by around 99% of its initial (undoped) value, together with clear absorption bands [21], where one of the transitions has the optimal value for an IB device [9], i.e. 0.72 eV above the VB maximum, thus demonstrating the suitability of N doped Cu_2O for IBSC applications.

In this study we use photoelectron spectroscopy and *in situ* ion implantation to demonstrate a simple and reliable nitrogen doping strategy in Cu_2O samples prepared by thermal oxidation. Furthermore, we demonstrate the robustness of this doping method by testing the influence of external factors, such as heat and exposure to air. Finally, our ion implantation is modeled using a Monte Carlo simulation program 'Stopping and Range of Ions in Matter' [22, 23] (as has been done for N implanted TiO_2 [24]), in order to estimate the implantation depth as a function of ion kinetic energy.

2. Methods

Cu_2O sheets were produced by thermal oxidation of 1 cm × 1 cm Cu foil sheets (0.127 mm thick, 99.99%, Alfa Aesar). The copper sheets were heated up to 1025 °C with a rate of 20 °C min^{-1} in a flux of Ar, at atmospheric pressure, and annealed for 60 min. Air was then introduced to the furnace for 120 min, and the samples were annealed again in flowing Ar for a further 120 min, to increase the Cu_2O grain dimensions, followed by slow temperature decrease at the rate of 20 °C min^{-1} back to RT.

Samples were introduced into an ultra high vacuum (UHV) chamber for further preparation and analysis. Immediately prior to insertion, samples were etched with a solution of HNO_3 (50–65%), followed by rinsing in ethanol [5, 25] in order to remove the surface layer of CuO which forms on exposure to air. Samples were further cleaned in vacuum by mild cycles of Ar^+ sputtering and annealed at 650 °C in order to desorb any contaminants which may have been absorbed during exposure to atmosphere.

N^+ ion implantation was carried out using an ion gun with an accelerating potential of up to 5 kV, a N_2 pressure of 3.8×10^{-6} Torr and an emission current of 10 mA, for 30 min. Following implantation, samples were incrementally annealed and/or exposed to air. At every stage in the experiment, x-ray and Ultraviolet photoemission spectroscopy (XPS and UPS) were used for chemical analysis as well as to monitor the electronic doping.

Photoemission experiments were carried out using both a home XPS/UPS instrument (shown in figure 1), and the soft x-ray beamline at the Australian synchrotron [26]. In both cases, the in vacuum preparation and N^+ implantation were similar. Energy shifts are generally measured using home XPS/UPS, because the photon energy is precisely known. Synchrotron photoemission is primarily used to collect high quality data of minority species (i.e. the N 1s core level), which is below the detection limit of the home XPS instrument.

3. Results

In d-electrons systems such as Cu_2O, a group V atom, such as nitrogen, is expected to behave as an electron acceptor, thus creating a charge imbalance in the host, causing an initially undoped Cu_2O to become a *p*-type semiconductor. Such doping would be visible as a shift in the VB relative to the Fermi level (E_F); and this is directly observable using UPS. The accompanying change in the stoichiometry (i.e. N concentration) is directly observable (and quantifiable) using XPS, and hence these two techniques are highly complementary. On the

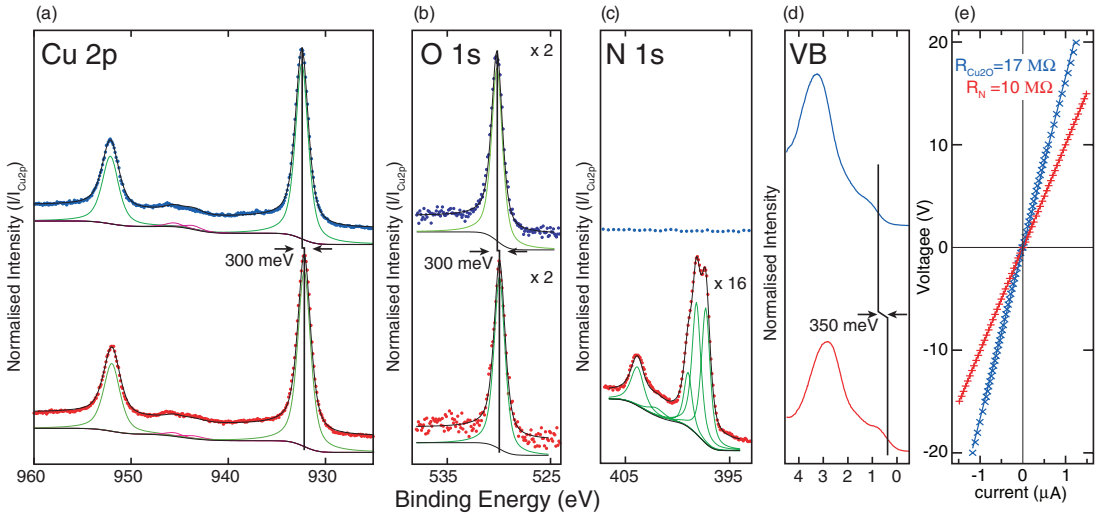

Figure 2. Cu_2O before and after N^+ implantation. (a)–(c), Cu 2p, O 1s and N 1s core levels, respectively. The O 1s and Cu 2p core levels are collected using an Mg kα x-ray anode with a well defined energy calibration (such that the energy shifts are precisely determined). The N 1s core level was below the detection limit of a home XPS, and is therefore collected using synchrotron radiation ($h\nu = 550$ eV). The intensity scales have been corrected for flux, integration time and photoionisation cross-section. (d) Valence band spectra collected with a He-Iα source ($h\nu = 21.2$ eV). (e) 2-contact current versus voltage measurements showing the sample resistance before (blue x) and after (red+) N implantation, together with a linear fit (blue and red solid lines, respectively). The gradient of the fit is also indicated: Before N implantation, $R_{Cu_2O} = 17\,M\Omega$, and after, $R_N = 10\,M\Omega$.

other hand, since a relatively low concentration of N can lead to a significant shift in the VB relative to E_F, UPS is significantly more sensitive in detecting the presence of small quantities of dopants (as compared to chemical quantification using XPS).

In figure 2(d), the VB position is shown both before and after N^+ implantation. Prior to ion implantation, the VB maximum is observed at a binding energy of $\approx$1 eV (measured relative to a metal Fermi level). After ion implantation, the VB maximum is shifted by 350 meV. This indicates a very significant change in the doping; with the Fermi level position moving significantly towards the top of the valence band relative to its initial position at approximately mid gap (i.e. intrinsic Cu_2O). Figures 2(a)–(c) shows the corresponding XPS acquisitions of the Cu 2p, O 1s, and N 1s core levels; due to doping, the O 1s and Cu $2p_{3/2}$ show shifts of 300 meV relative to the Fermi level, consistent with the shift of the VB. The N 1s core level is undetectable prior to ion implantation. Following implantation, a multi-component N 1s peak is detected. The total quantity of N present is found to be $\leqslant$7%. A 2-contact resistance measurement (with a probe separation of 0.5 mm), was carried out in vacuum, immediately before and after N implantation (figure 2(e)) and a significant reduction in the sample resistance was observed concomitant with the shift in the VB and core levels. The current versus voltage measurements are both well approximated by a straight line, with gradient (i.e. sample resistance) $16.65 \pm 0.06\,M\Omega$ and $10.05 \pm 0.01\,M\Omega$ before and after N implantation, respectively[6].

Although the total intensity is weak, the N 1s peak has been collected in high quality and fitted (see figure 2(c)). The fit reveals that at least 4 distinct components are present: 3 large components in the binding energy range 396–399 eV, and a broad, or perhaps multi-component structure at around $E_B = 404$ eV.

Following N implantation, a large variety of products are possible, the observation of a complex peak structure in the N 1s region is unsurprising. However, not all N species necessarily result in active p dopants. One family of possible products is CuN_x, where x may take a range of values, for example $x = 1/2$ corresponds to Cu_2N, i.e. substitutional doping of Cu_2O by replacement of the oxygen atom by an implanted nitrogen ion. CuN_2 and CuN_3 are both expected in the energy range $E_B = 396$–399 eV [27, 28], and additional CuN_x species are also possible [29, 30].

In addition to the CuN_x family formed by O substitution, CuN_xO_y species involving the addition of a nitrogen atom to the Cu_2O host are also a possibility. Various combinations of x and y are feasible, and would appear at an energy of $E_B \approx 404$ eV [27, 28], where, indeed a peak is observed.

The N ion source used in this work also produces a fraction of ionised molecular nitrogen, i.e. N_2^+, thus the implantation of molecular N_2 is also possible. Recent experimental evidence [31] and first principles calculations [32] indicate that not only is $(N_2)_{Cu}$ (i.e. N_2 substituted at a Cu site) a feasible product with a low formation energy, it gives rise to a shallow acceptor level and is perhaps the most feasible origin of p type doping. The binding energy of N_2 substituted at a Cu site is not clear, but in GaN and InN, implanted N_2^+ is reported at $E_B \approx 405$ eV [33], consistent with our $E_B \approx 404$ eV peak.

[6] Since 2-contact resistance measurements also contain the contact resistance [36], the true sample resistance is presumably much smaller than these measurements indicate.

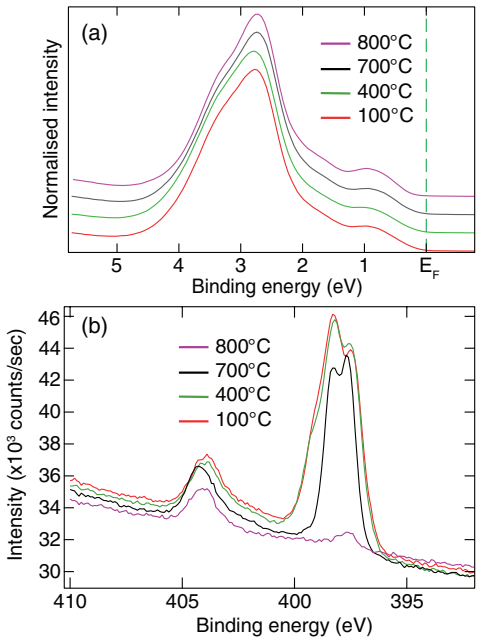

Figure 3. Thermal treatment of nitrogen doped Cu_2O. (a) Valence band spectra following a range of annealing temperatures, collected using synchrotron radiation ($h\nu = 410$ eV) (b) Evolution of the N 1s core level with annealing temperature ($h\nu = 550$ eV).

In addition to the data plotted in figure 3, the N 1s peak was also measured using higher photon energy (i.e. less surface sensitive), and shows a relative reduction of the lower binding energy (CuN_x) species, indicating that they are closer to the surface than the higher binding energy (CuN_xO_y or $(N_2)_{Cu}$) species. This is consistent with the notion that substitution of Cu_2O to form Cu_2N (with the release of oxygen gas) is only feasible at the surface, whereas capture of N, without the release of O (to form CuN_xO_y) is feasible at all depths.

It is clear from the UPS and XPS data presented in figure 2 that N^+ implantation causes Cu_2O to change from being nearly intrinsic, to becoming highly *p*-doped; ≈350 meV of doping is observed, consistent with the measured nitrogen concentration of ⩽7%. However, in order for this doping to be useful in device applications, it is also important to investigate its robustness.

To check the stability of the implanted N with the increase of temperature, the implanted sample was annealed incrementally, for 10 min at each temperature step up to 800 °C, as shown in figure 3. UPS measurements of the VB were performed at each temperature step, and are plotted in figure 3(a), as well as N 1s core level, shown in figure 3(b). It is clear from figure 3 that neither the N 1s core level, nor the VB spectra show any significant change until at least 400 °C is reached. This already implies that the doping is sufficiently robust to withstand any normal application environment.

Upon continued annealing, the largest N 1s components (in the binding energy range 396–400 eV) rapidly reduces, however, this is not accompanied by a significant change in the VB position. This indicates that the CuN_x nitrogen species which give rise to these low binding energy components do not actively contribute as *p* dopants, consistent with [32]. The higher binding energy N 1s component (i.e. $(N_2)_{Cu}$ or CuN_xO_y) at $E_B \approx 404$ eV only decreases (and starts to shift) when the sample temperature exceeds 700 °C, indicating that this component is primarily responsible for the *p*-type doping, and it is strongly bonded and therefore cannot be removed by heating until the temperature approaches that required to decompose the host Cu_2O. In short, the implanted N in general, and the active dopant species in particular, are very robust against extremes of temperature.

Since the ion implantation and photoemission measurements are performed without exposure of the sample to air, it is important to perform an additional test to see if the ion implanted sample is robust against exposure to typical atmospheric contaminants. Therefore, the doped samples were purposely exposed to air for 2 h, before being re-introduced into the UHV measurement chamber, and remeasured (without any further preparation). Figure 4 shows the VB measurement of an ion implanted sample, both before and after exposure to air. A small shift in the VB maximum is seen; this may be due to the re-formation of a surface oxide or the absorption of an atmospheric dopant (such as water). On the other hand, the Cu_2O sample is known to form a surface CuO layer upon exposure to air [34], and our quantitative analysis of the Cu 2p and O 1s core level intensities, shows a reduction in the Cu:O ratio of 25%. We therefore infer that the small shift in the VB maximum following air exposure is most likely due to the re-formation of surface CuO. The subsurface implanted dopants are unaffected by this change is surface oxidation.

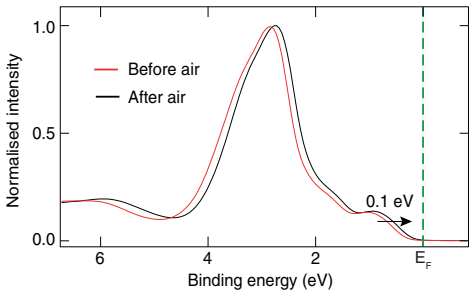

Figure 4. Valence band spectra of N implanted Cu_2O before and after being exposure to atmosphere, collected using synchrotron radiation ($h\nu = 100$ eV).

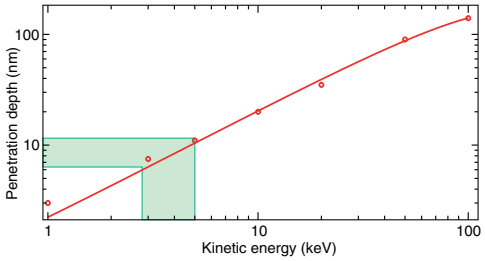

Figure 5. Results from Monte Carlo simulations of nitrogen ion implantation. The N^+ penetration depth is plotted as a function of the ion's kinetic energy, and the green band indicates the energy range used in our experimental work.

4. Model of implantation depth

We have shown that N^+ implantation in Cu_2O results in strong *p*-doping of the host. Furthermore, it appears that the active dopant species is incorporated N (rather than weakly surface-bonded N). This is not surprising since the kinetic energy of the ions is sufficiently high for them to penetrate the sample surface. On the other hand, the penetration depth cannot be very large because the N 1s core level is clearly observable using XPS, which is known to be very surface sensitive [35]. We have therefore carried out a simple Monte Carlo simulation in order to model the ion implantation.

The simulation we have used is for amorphous targets [22], however, it is a good approximation here since the top layers of our Cu_2O sample show no crystalline order (i.e. no ordering was observed with low energy electron diffraction).

In our experiments, we have used an accelerating potential of 3–5 kV, but the simulations were carried out for a larger energy range (i.e. 1 to 100 keV), as shown in figure 5, in order to demonstrate the possible depth range achievable with this approach. As can be seen from the figure, the simulation indicates an implantation depth of 8.5 ± 2.5 nm for the 3 to 5 keV ions used in our experiments, and indicates that this depth could be adjusted from $\approx$3 to 100 nm by tuning the accelerating potential over a larger, but realistic, range.

5. Conclusion

We have demonstrated a simple method for controllable *p*-doping of Cu_2O using implantation of low energy N^+ ions. XPS and UPS measurements show that very strong *p*-doping can be achieved by incorporating $\leqslant$7% N into the Cu_2O host: the approximately mid-gap position of the Fermi level in the initially un-doped Cu_2O is shifted 350 meV closer to the VB maximum. Analysis of the N 1s core level components, and their robustness to elevated temperatures indicates that the active dopant species is $(N_2)_{Cu}$ (i.e. N_2 substituted at a Cu site) or CuN_xO_y, rather than CuN_x (i.e. N substituted at an O site), although other co-ordinations of N may also be present.

Our study also shows that ion implanted Cu_2O is very robust and can survive extremes of temperature without significant modification of the electrical properties. It also survives exposure to atmospheric contaminants, although the surface appears to revert to CuO.

A Monte Carlo simulation indicates that the ion implantation depth in these experiments is 8.5 ± 2.5 nm, and that implantation depths of up to $\approx$100 nm would be possible by increasing the ion energy.

Finally, the materials used here are safe, abundant and non-toxic. The method used for the growth of Cu_2O (i.e. annealing Cu foil and exposing it to air), and the method used for the N^+ implantation are simple and would be

cheap to implement on a large scale. Demonstrating robust controllable doping using such materials and methods is an important step in the realization of affordable intermediate band photovoltaics.

Acknowledgments

This project was partially funded by the Research Council of Norway through project number 240466 'OX-IB' in the *energix* program. This research was partially undertaken on the soft x-ray beamline at the Australian Synchrotron, Victoria, Australia.

References

[1] Rai B 1988 *Sol. Cells* **25** 265
[2] Jolk A, Jörger M and Klingshirn C 2002 *Phys. Rev.* B **65** 245209
[3] Wang E, Trivich D, Sawalha H and Thomas G 1976 *Heliotechnique and Development* vol 1 (Cambridge: Development Analysis Associates) pp 643–50
[4] Olsen L, Addis F and Miller W 1982 *Sol. Cells* **7** 247
[5] Mittiga A, Salza E, Sarto F, Tucci M and Vasanthi R 2006 *Appl. Phys. Lett.* **88** 163502
[6] Raebiger H, Lany S and Zunger A 2007 *Phys. Rev.* B **76** 045209
[7] Minami T, Nishi Y and Miyata T 2016 *Appl. Phys. Express* **9** 052301
[8] Shockley W and Queisser H J 1961 *J. Appl. Phys.* **32** 510
[9] Luque A and Martí A 1997 *Phys. Rev. Lett.* **78** 5014
[10] Marti A, Cuadra L and Luque A 2000 *Conf. Record of the 28th IEEE Photovoltaic Specialists Conf.* p 940
[11] Walukiewicz W, Yu K M, Wu J, Ager J W, Shan W, Scrapulla M A, Dubon O D and Becla P 2005 *MRS Proc.* 865 F5.7 (http://dx.doi.org/10.1557/PROC-865-F5.7)
[12] Yang X, Nematollahi M, Gibson U N and Reenaas T W 2013 *2013 IEEE 39th Photovoltaic Specialists Conf.* pp 2494–7
[13] Mazzola F, Nematollahi M, Li Z S, Cooil S, Yang X, Reenaas T W and Wells J W 2015 *Appl. Phys. Lett.* **107** 192104
[14] Luque A, Martí A, Antolín E and Tablero C 2006 *Physica* B **382** 320
[15] Papadimitriou L, Economou N and Trivich D 1983 *Solid-State Electron.* **26** 767
[16] Cai X M *et al* 2015 *Appl. Phys. Lett.* **107** 083901
[17] Han X and Tao M 2009 *34th IEEE Photovoltaic Specialists Conf.* (IEEE) p 002086
[18] Ishizuka S, Kato S, Maruyama T and Akimoto K 2001 *Japan. J. Appl. Phys.* **40** 2765
[19] Nakano Y, Saeki S and Morikawa T 2009 *Appl. Phys. Lett.* **94** 76
[20] Li H, Pu C, Ma C, Li S, Dong W, Bao S and Zhang Q 2011 *Thin Solid Films* **520** 212
[21] Malerba C, Azanza Ricardo C L, D'Incau M, Biccari F, Scardi P and Mittiga A 2012 *Sol. Energy Mater. Sol. Cells* **105** 192
[22] Biersack J P and Haggmark L 1980 *Nucl. Instrum. Methods* **174** 257
[23] Ziegler J F, Ziegler M D and Biersack J P 2010 *Nucl. Instrum. Methods Phys. Res.* B **268** 1818
[24] Batzill M, Morales E H and Diebold U 2007 *Chem. Phys.* **339** 36
[25] Ievskaya Y, Hoye R, Sadhanala A, Musselman K and MacManus-Driscoll J 2015 *Sol. Energy Mater. Sol. Cells* **135** 43
[26] Cowie B C C, Tadich A and Thomsen L 2010 *AIP Conf. Proc.* **1234** 307
[27] Bertóti I 2012 *Catalysis Today* **181** 95
[28] Wagner C, Riggs W, Davis L and Moulder J 1979 *Handbook of X-Ray Photoelectron Spectroscopy* ed G Mullenberg (Minnesota: Perkin-Elmer Corporation)
[29] Prabhawalker P D, Kothari D C, Nair M R and Raole P M 1985 *Nucl. Instrum. Methods Phys. Res.* B **7** 147
[30] Liu Z Q, Wang W J, Wang T M, Chao S and Zheng S K 1998 *Thin Solid Films* **325** 55
[31] Wang Y, Ghanbaja J, Horwat D, Yu L and Pierson J F 2017 *Appl. Phys. Lett.* **110** 131902
[32] T-Thienprasert J and Limpijumnong S 2015 *Appl. Phys. Lett.* **107** 221905
[33] Bozanic A, Majlinger Z, Petravic M, Gao Q, Llewellyn D, Crotti C and Yang Y W 2008 *J. Vac. Sci. Technol.* A **26** 592
[34] Platzman I, Brener R, Haick H and Tannenbaum R 2008 *J. Phys. Chem.* C **112** 1101
[35] Seah M P and Dench W A 1979 *Surf. Interface Anal.* **1** 2
[36] Hofmann P and Wells J W 2009 *J. Phys.: Condens. Matter* **21** 013003